Title

Optic Nerve Head Deformation in Glaucoma: A Prospective Analysis of Optic Nerve Head Surface and Lamina Cribrosa Surface Displacement

Journal

Ophthalmology, 122(7)

ISSN

0161-6420

Authors

Wu, Z
Xu, G
Weinreb, RN
et al.

Publication Date

2015-07-01

DOI

10.1016/j.ophtha.2015.02.035

Peer reviewed

CrossMark

American Academy of Ophthalmology
The Eye M.D. Association

Optic Nerve Head Deformation in Glaucoma

A Prospective Analysis of Optic Nerve Head Surface and Lamina Cribrosa Surface Displacement

Zhongheng Wu, BM,[1] Guihua Xu, BM,[1] Robert N. Weinreb, MD,[2] Marco Yu, PhD,[1,3] Christopher K.S. Leung, MD, MBChB[1]

Purpose: To evaluate long-term, longitudinal displacement of the optic nerve head (ONH) and anterior lamina cribrosa surfaces in glaucoma patients imaged with spectral-domain optical coherence tomography (SD OCT).

Design: Prospective study.

Participants: A total of 173 eyes of 108 subjects (88 with glaucoma and 20 normal subjects) followed for a mean of 5.3 years.

Methods: The optic disc was imaged with SD OCT at approximately 4-month intervals, and the ONH surface depth (ONHSD), anterior lamina cribrosa surface depth (ALCSD), and prelaminar tissue thickness (PTT) were measured. The reproducibility coefficients of ONHSD, ALCSD, and PTT were calculated from 2 baseline measurements of the glaucoma group. Change in ONHSD/ALCSD/PTT was confirmed when the differences between the first baseline and the latest 2 consecutive follow-up visits were greater than the corresponding reproducibility coefficient. Factors associated with ONHSD and ALCSD changes were identified with linear mixed modeling.

Main Outcome Measures: Proportion of eyes with ONHSD/ALCSD change.

Results: Within the glaucoma group, 23.9% (33 eyes) had confirmed ONHSD change (15.2% with posterior and 8.7% with anterior displacement) and 24.6% (34 eyes) had confirmed ALCSD change (12.3% with posterior and 12.3% with anterior displacement). Some 9.4% (13 eyes) showed a decrease in PTT, and 2.2% (3 eyes) showed an increase in PTT. The specificity for detection of ONHSD/ALCSD/PTT change was 91.4% (95% confidence interval [CI], 77.6-97.0), 82.9% (95% CI, 67.3-91.9), and 94.3% (95% CI, 81.4-98.4), respectively. There were no significant differences in the proportion of eyes with visual field progression or history of filtration surgery between the groups with anterior and posterior displacement of ONH/anterior laminar surfaces ($P \geq 0.678$). For each millimeter of mercury increase in the average intraocular pressure (IOP) during follow-up, the ONH and anterior laminar surfaces displaced posteriorly by 1.6 μm and 2.0 μm, respectively. An older age was associated with a decrease in magnitude of posterior displacement of the ONH and anterior laminar surfaces ($P \leq 0.009$).

Conclusions: The ONH and anterior laminar surfaces displaced not only posteriorly but also anteriorly (with reference to Bruch's membrane opening) in a significant portion of glaucoma patients. The magnitude of change was related to age and the averaged IOP during follow-up. *Ophthalmology 2015;122:1317-1329 © 2015 by the American Academy of Ophthalmology.*

Study of the optic nerve head (ONH) structures, including the lamina cribrosa (LC), is relevant to understanding the mechanisms of retinal ganglion cell degeneration in glaucoma and devising new diagnostic and therapeutic strategies. The advent of spectral-domain optical coherence tomography (SD OCT), adaptive optics optical coherence tomography (OCT), and adaptive optics confocal scanning laser ophthalmoscopy has improved the assessment of the LC and Bruch's membrane opening (BMO).[1–3] Although challenges remain in accurately delineating the posterior boundary of the LC and visualizing structures obscured by the retinal vasculature, SD OCT affords reliable measurement of the optic nerve head surface depth (ONHSD) and anterior lamina cribrosa surface depth (ALCSD), commonly defined by the perpendicular distances from a line joining the ends of BMO, or from the BMO plane fit in 3 dimensions, to the ONH surface and the anterior LC surface, respectively.[4–12] Strouthidis et al[5] demonstrated a significant increase in ALCSD over a mean follow-up of 2.8 months in 9 rhesus macaques induced with experimental glaucoma and proposed that ONH imaging and measurements would be useful in longitudinal follow-up of patients with glaucoma.[5] Clinical studies have demonstrated anterior displacement of the ONH and anterior LC surfaces after trabeculectomy[9–11] and posterior displacement of the

http://dx.doi.org/10.1016/j.ophtha.2015.02.035
ISSN 0161-6420/15

ONH surface during acute intraocular pressure (IOP) elevation.[12] However, it remains unclear whether displacement of the ONH and LC surfaces can be observed clinically with serial measurements during the course of glaucoma progression. If present, moreover, it is unknown whether such displacement would be anterior or posterior. Current knowledge of deformation of the ONH and anterior LC surfaces in glaucoma is primarily derived from modeling[13–15] and experimental studies.[4–8] Therefore, a long-term clinical study is germane to address the nature of chronic, progressive deformation of the ONH in glaucoma. In this study, we analyzed the ONH imaged with SD OCT at approximately 4-month intervals in 173 eyes of 88 patients with glaucoma and 20 normal subjects followed for an average of 5.3 years. The objective of this prospective study was to investigate the longitudinal profiles of ONHSD/ALCSD and their association with IOP during longitudinal follow-up.

Methods

Subjects

A total of 132 subjects, including 93 with glaucoma and 39 normal healthy individuals, were consecutively enrolled and followed from March 2008 to September 2014 at the University Eye Center, the Chinese University of Hong Kong. After excluding 13 eyes of 13 patients with glaucoma and 43 eyes of 24 normal subjects because of indiscernible anterior LC surface in at least 1 B-scan in the baseline and follow-up visits (the presence of small optic cups or thick neuroretinal rim precluded the detection of the anterior LC surface, and more eyes were therefore excluded in the normal group), 138 eyes of 88 patients with glaucoma and 35 eyes from 20 normal subjects were included for analysis. All subjects had a complete ocular examination, including measurement of visual acuity, IOP, axial length, and refraction. Gonioscopy and fundus examination were performed. The optic discs were examined with slit-lamp biomicroscopy. Color optic disc stereophotographs were obtained. Included eyes had visual acuity $\geq$20/40 with longitudinal follow-up of at least 48 months. Eyes were excluded if there was evidence of macular disease, neurologic disease, and refractive or retinal surgery. Patients with glaucoma were identified on the basis of the presence of characteristic optic disc/retinal nerve fiber layer (RNFL) changes with corresponding visual field abnormalities in at least 1 eye, regardless of the level of IOP. Normal individuals had IOP $<$22 mmHg during all follow-up visits and no evidence of ocular disease, optic disc/RNFL abnormalities, or major systemic illness. Both eyes had optic disc and RNFL imaging with SD OCT, and visual field examination also was performed at the same visit at approximately 4-month intervals. Patients were managed during follow-up at the discretion of the attending ophthalmologists with reference to their target IOP. The study was conducted in accordance with the ethical standards stated in the 1964 Declaration of Helsinki and approved by local research ethics committee with informed consent obtained.

Optical Coherence Tomography Imaging

The optic disc was imaged with the Spectralis OCT (Heidelberg Engineering, GmbH, Dossenheim, Germany; super-luminescent diode laser center wavelength: 870 nm; scan speed: 40 000 A-scans per second) using 6 radial scan lines, each with 1024 A-scans, equally spaced at 30°. Because the study was initiated before the introduction of enhanced-depth imaging (EDI),[16] the baseline OCT scans were obtained without using the EDI mode. After June 2011, all OCT scans were then acquired using both EDI and non-EDI modes (both based on 6 radial scan lines). For this study, we included only non-EDI baseline and follow-up scans with clear visibility of the ONH and anterior LC surfaces. The RNFL was imaged with a circle scan comprising 1536 A-scans with a diameter of approximately 3.45 mm. The anterior and posterior boundaries of the RNFL were automatically segmented by the built-in software, and the global RNFL thickness was measured. Four eyes had RNFL segmentation errors, and the RNFL boundaries were manually edited by the instrument software. Both the radial scans and the circle scan were positioned at the optic disc center on the basis of the operator estimation of the clinical disc margin while the eye-tracking system was activated. Follow-up OCT scans were acquired with reference to the locations of the registered baseline scan using the eye-tracking technology. Fifteen B-scans at the same location were obtained and automatically averaged by the built-in software to increase the image signal-to-noise ratio. Averaging was applied to both radial and circle scans. All OCT volumes included in the study had a scan quality score of at least 20. The optic disc was also imaged with the Cirrus HD-OCT (Carl Zeiss Meditec, Dublin, CA; super-luminescent diode laser wavelength: 840 nm; scan speed: 27 000 A-scans per second) at the same baseline visit using the optic disc cube scan (200 $\times$ 200 pixels) for measurement of the BMO area. The built-in software automatically detected the BMO in each of the B-scans and computed the BMO area. Cirrus HD-OCT BMO area measurement has been shown to have high repeatability.[17] All Cirrus HD-OCT RNFL analyses had a signal strength of $\geq$7 without any motion artefacts.

Measurement of Optic Nerve Head Surface Depth, Anterior Lamina Cribrosa Surface Depth, and Prelaminar Tissue Thickness

Measurement of ONHSD, ALCSD, and prelaminar tissue thickness (PTT) was performed in the Spectralis OCT B-scans using a customized computer program developed in Matlab (R2010a, the MathWorks, Inc., Natick, MA). All B-scans (1:1 pixel in scale) were exported as image files after setting the baseline scan as reference. The program measured the ONHSD, ALCSD, and PTT on manual detection and tracing of the BMO, internal limiting membrane, ONH surface, and anterior LC surfaces. The scaling factor (micrometers/pixel) for individual B-scans was extracted from the built-in software and applied in the customized program for calculation of ONHSD, ALCSD, and PTT. The tracing of the internal limiting membrane and ONH surface was assisted by the piecewise cubic Hermite interpolation polynomial (highlighted in green in Fig 1). The ONHSD (Fig 1B) represented the perpendicular distances from the reference line, a line joining the BMO (highlighted in pink in Fig 1), to the ONH surface (i.e., the perpendicular distances linking individual pixels of the reference line and the ONH surface were measured in the B-scan image [1024 $\times$ 496 pixels]). The ALCSD (Fig 1C) represented the perpendicular distances from the reference line to the detectable anterior LC surface (highlighted in orange in Fig 1), which was manually identified as the intersection between the horizontal moderate-intensity signal below the disc surface and the high-intensity vertical striations.[5] The PTT (Fig 1D) was the distance between the ONH and the detectable anterior LC surface (i.e., the differences between the ALCSD and the ONHSD along the detectable pixels of the anterior

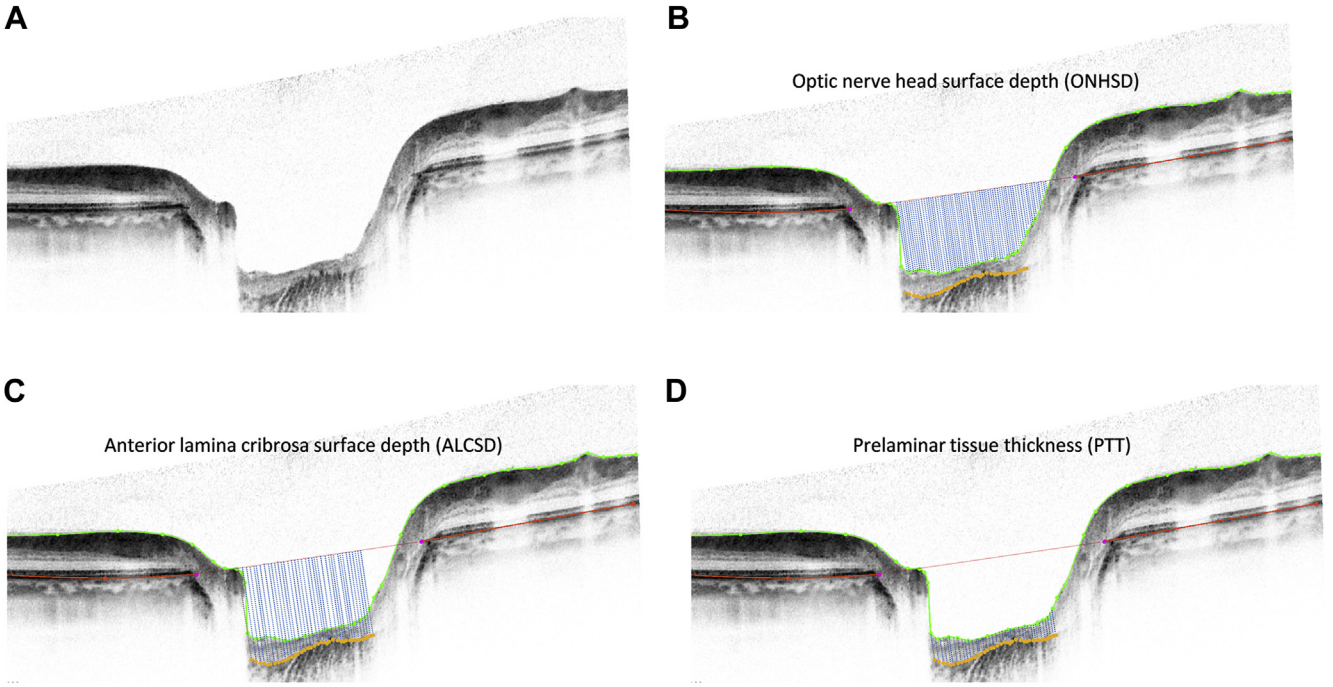

Figure 1. An optical coherence tomography (OCT) optic disc image **(A)** for measurement of the optic nerve head surface depth (ONHSD) **(B)**, anterior lamina cribrosa surface depth (ALCSD) **(C)**, and prelaminar tissue thickness (PTT) **(D)** after manual detection of the Bruch's membrane opening (BMO) (*pink dots*), internal limiting membrane/ONH surface (*green*), and anterior lamina cribrosa (LC) surface (*orange*). The reference line (*pink*) is a line joining the BMO. The ONHSD represents the perpendicular distances from the reference line to the ONH surface (the *blue lines* are for illustrative purpose and do not represent all the lines the software measured). The ALCSD represents the perpendicular distances from the reference line to the anterior LC surface. The PTT represents the distance between the ONH and the anterior LC surfaces. The retinal pigment epithelium/Bruch's membrane is highlighted in *red*.

laminar surface). Because the visibility of the anterior LC surface was often incomplete due to the presence of retinal vasculature, the ALCSD and PTT were only measured with reference to the locations where the anterior LC surface was visible in the B-scans. The ONHSD, ALCSD, and PTT of an optic disc were calculated from the averages of the 6 radial B-scans. The OCT scans were included for change analysis only when the ONH and the anterior LC surfaces were visible, and the ONHSD/ALCSD/PTT measurements were made in all of the 6 B-scans for each of the baseline and the latest 2 consecutive follow-up visits for an individual eye. Each of the delineated distances at the ONH and anterior LC surfaces was weighted in proportion to its distance from the center point between the pair of BMO points (the peripheral portion carried a greater weight than the central portion):

$$\bar{y} = \frac{\sum_{i=1}^{6} \bar{y}_i}{6}$$

$$\bar{y}_i = \frac{\sum_{j=1}^{n_i} d_{ij} y_{ij}}{\sum_{j=1}^{n_i} d_{ij}}$$

where $\bar{y}$ represents the average measurement of ONHSD, ALCSD, or PTT of an eye, which is given by averaging the mean values of each of the 6 radial B-scans $\bar{y}_i$ (for $i = 1, 2, \ldots, 6$); $\bar{y}_i$ is the weighted average of the distance measure, y_{ij}, obtained by point j in B-scan i with a weighting given by its distance from the BMO center point, d_{ij}. The weightings were given to account for the area represented by the samples because the radial scan pattern underrepresented the periphery relative to the center.

Change Analysis of Optic Nerve Head Surface Depth, Anterior Lamina Cribrosa Surface Depth, and Prelaminar Tissue Thickness

Optical coherence tomography scans obtained from the baseline and the latest 2 consecutive follow-up visits were measured for detection of change. Two baseline measurements (separated by 4 months) of 138 eyes of 88 patients with glaucoma were used to calculate the reproducibility coefficients of ONHSD, ALCSD, and PTT. The reproducibility coefficient was defined as $1.96 * \sqrt{2} * \mathrm{Sw}$ (where Sw represents within-subject standard deviation [SD]),[18,19] which is an estimate of the limit within which 95% of the differences between 2 measurements are made at random on the same subject. The width of the 95% confidence interval (CI) for the within-subject SD is given by $1.96 * (\mathrm{Sw}/\sqrt{[2n(m-1)]})$ on either side of the estimate (where n is the number of subjects and m is the number of observations). By including 2 measurements from 138 eyes, the width of the 95% CI of Sw was therefore 11.8% of the $\mathrm{Sw}(1.96/\sqrt{[2 * 138]} = 11.8\%)$. In other words, the 95% CIs of the reproducibility coefficients were relatively narrow. The ONHSD/ALCSD/PTT change was confirmed when the differences between the first baseline and the latest 2 consecutive follow-up visit were greater than the respective reproducibility coefficients. The time when significant change was first detected was recorded.

Table 1. Demographics, Visual Field, and Optical Coherence Tomography Measurements of the Normal and Glaucoma Groups

	Normal Subjects	Patients with Glaucoma	P Value*
Subjects/eyes	20/35	88/138	/
Baseline age (yrs)	54.1±7.0 (35–65)	49.5±14.7 (18–76)	<0.001
Gender (male/female)	6/14	48/40	<0.001
Duration (yrs)	5.1±0.5 (4.0–6.0)	5.4±0.5 (4.0–6.4)	0.937
Refractive error (D)	0.14±1.66 (−4.25 to 2.75)	−3.66±4.10 (−13.00 to 3.75)	<0.001
Axial length (mm)	23.8±1.0 (21.9–25.8)	25.2±1.9 (21.8–30.1)	<0.001
Baseline MD (dB)	−0.14±1.08 (−2.75 to 2.06)	−8.40±8.60 (−32.81 to 0.37)	<0.001
Baseline BMO area (mm^2)	1.99±0.27 (1.56–2.57)	2.08±0.45 (1.17–3.56)	0.494
Baseline global RNFL thickness (μm)	99.4±9.9 (77–130)	68.9±17.6 (30–121)	<0.001
Baseline ONHSD (μm)	169.6±68.8 (31.8–332.9)	242.1±78.7 (59.3–516.0)	<0.001
Baseline ALCSD (μm)	391.5±66.6 (256.0–570.9)	452.6±95.4 (224.3–726.6)	<0.001
Baseline PTT (μm)	196.8 ±76.7 (93.5–388.5)	144.1±48.4 (33.8–294.7)	<0.001
Latest ONHSD (μm)	167.3±67.8 (28.0–325.6)	246.7±78.3 (63.4–531.7)	<0.001
Latest ALCSD (μm)	387.7±68.2 (221.9–580.0)	453.6±96.0 (226.3–757.2)	<0.001
Latest PTT (μm)	198.9±72.6 (98.0–382.8)	137.2±45.9 (42.4–294.5)	<0.001

ALCSD = anterior lamina cribrosa surface depth; BMO = Bruch's membrane opening; D = diopters; dB = decibels; IOP = intraocular pressure; MD = mean deviation; ONHSD = optic nerve head surface depth; PTT = prelaminar tissue thickness; RNFL = retinal nerve fiber layer.
*Comparisons were performed using linear mixed modeling except for "gender," for which chi-square was used.

The same criteria for detection of change were applied in both the glaucoma and normal groups.

Visual Field Examination

Standard white-on-white automated perimetry was performed with the Humphrey Field Analyzer II-i (Carl Zeiss Meditec) (SITA standard 24-2) during the follow-up visits. The fixation losses and false-positive and false-negative errors were <20% for all visual fields. A visual field defect had ≥3 significant ($P < 0.05$) nonedge contiguous points (≥1 with $P < 0.01$) on the same side of horizontal meridian in the pattern deviation plot. A visual field defect had to be confirmed with ≥2 consecutive examinations.

Analysis of Visual Field Progression

Visual field progression was defined using the Early Manifest Glaucoma Trial criteria[20] as reported in the Guided Progression Analysis in the Humphrey Field Analyzer (Carl Zeiss Meditec). Progression was defined when there were ≥3 points that showed a significant change (greater than the test–retest variabilities) compared with 2 baseline examinations (separated by ~4 months in this study) for at least 2 consecutive tests (i.e., "likely progression" or "possible progression" was noted in the Guided Progression Analysis printout in the latest follow-up visit).

Intraocular Pressure Measurement

The dynamic contour tonometer (DCT) (Pascal; Swiss Microtechnology AG, Port, Switzerland) was used to measure the IOP in the glaucoma patients because the DCT IOP measurement has been shown to be less dependent on central corneal thickness and corneal biomechanical properties compared with Goldmann applanation tonometry.[21–23] Because the degree of deformation of the ONH/anterior LC surfaces in patients with glaucoma is likely related to the ocular biomechanical properties, the DCT IOP would be a more appropriate measure to investigate the relationship between IOP and ONHSD/ALCSD changes. The principle of DCT has been described.[24] In brief, the contour of the tonometer matched with the contour of the cornea, and the IOP was measured by a pressure sensor at the tip of the tonometer. The duration of recording for each IOP measurement was approximately 5 seconds. Two measurements with a quality score between 1 and 3 (as recommended by the manufacturer) were obtained for each eye, and the average was calculated. The diastolic IOP was used in the analysis. The average IOP and the SD of IOP during the follow-up of individual eyes were evaluated.

Statistical Analysis

Statistical analyses were performed with Stata version 12.0 (StataCorp LP, College Station TX). Differences in optic disc, RNFL, and visual field measurements between the normal and glaucoma groups were compared with linear mixed modeling, adjusting for the correlation between fellow eyes. Post hoc power calculation revealed the current sample size had a power of 82.2%, 83.3%, and 83.8% to detect an absolute difference of 6 μm for ONHSD, 8 μm for ALCSD, and 5 μm for PTT, respectively, at an alpha of 5%. The agreement of anterior/posterior displacement between the ONH and the anterior LC surfaces was evaluated with Cohen's kappa statistics. A value between 0.0 and 0.2 indicates slight agreement, 0.21 and 0.40 is fair, 0.41 and 0.60 is moderate, 0.61 and 0.80 is substantial, and 0.81 and 1 is almost perfect agreement.[25] The association between ONH/anterior LC surface displacement (the average of the 2 latest follow-up ONHSD/ALCSD measurements minus the average of the 2 baseline ONHSD/ALCSD measurements) and the following parameters, including average IOP during the follow-up, SD of IOP during the follow-up, baseline age, BMO area, axial length, global RNFL thickness, and history of filtration surgery (fixed effects), were evaluated with linear mixed modeling, with eye nested in subject (random effects). The coefficient of determination (R^2) of the fixed effects in the linear mixed modeling between change in ALCSD and change in ONHSD/PTT was calculated with reference to Nakagawa and Schielzeth.[26] Residual diagnostics had been performed to confirm the normality assumption for the random effects (evaluated by best linear unbiased predictor) and residuals of the linear mixed models. $P < 0.05$ was considered statistically significant.

Results

A total of 138 eyes of 88 patients with glaucoma and 35 eyes of 20 normal individuals followed for a mean of 5.3 years (range,

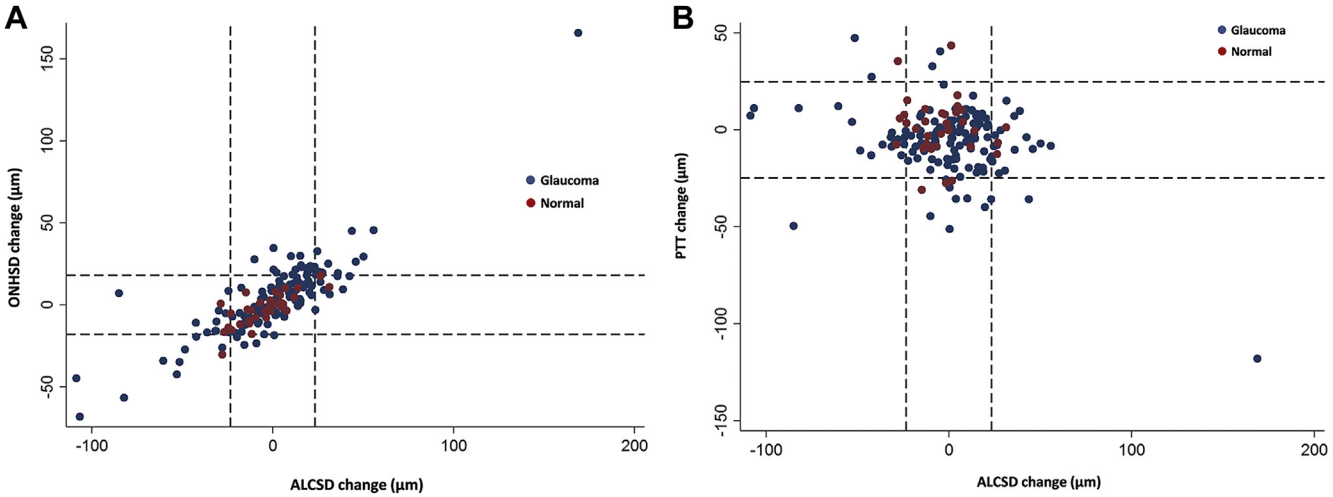

Figure 2. Scatter plots showing **(A)** the association between change in optic nerve head surface depth (ONHSD) (the mean of the latest 2 minus the mean of 2 baseline ONHSD measurements) and change in anterior lamina cribrosa surface depth (ALCSD) (the mean of the latest 2 minus the mean of 2 baseline ALCSD measurements); and **(B)** the association between change in prelaminar tissue thickness (PTT) (the mean of the latest 2 minus the mean of 2 baseline PTT measurements) and change in ALCSD (the mean of the latest 2 minus the mean of 2 baseline ALCSD measurements). The *vertical* and *horizontal dash lines* represent the reproducibility coefficient limits of the corresponding parameters. *Blue* — eyes from the glaucoma group; *red* — eyes from the normal group.

4.0—6.4 years) were included for analysis. At the baseline examination, there were 55.8% mild (mean deviation [MD] ≥ -6 decibels [dB]), 20.3% moderate (-6 dB $>$ MD > -12 dB), and 23.9% advanced (MD ≤ -12 dB) glaucomatous eyes. Thirty eyes (21.7%) had possible or likely visual field progression (in which 15, 12, and 3 eyes had mild, moderate, and advanced glaucoma, respectively), and 17 eyes (12.3%) had likely progression (in which 7, 8, and 2 eyes had mild, moderate, and advanced glaucoma, respectively) by the Early Manifest Glaucoma Trial criteria. The demographics, visual field, and OCT ONH measurements are shown in Table 1. The ONHSD and ALCSD were significantly greater and the PTT was significantly smaller in the glaucoma group compared with the normal group at both the baseline and latest follow-up visits ($P < 0.001$). The reproducibility coefficients of ONHSD, ALCSD, and PTT were 18.0 μm, 23.4 μm, and 24.8 μm, respectively.

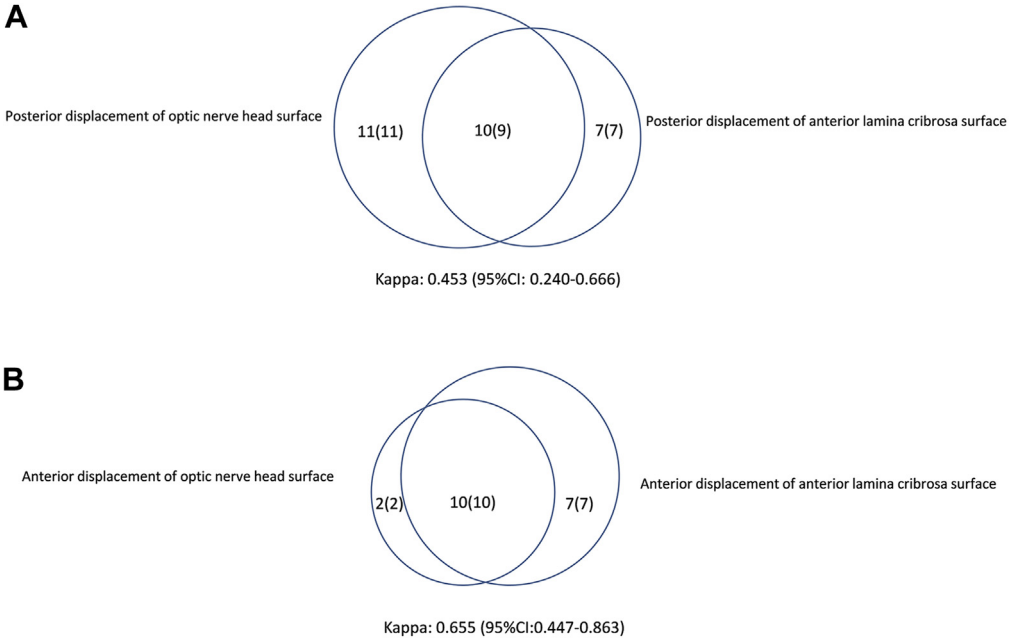

Figure 3. Venn diagram showing the number of eyes (the number of patients) with anterior **(A)** and posterior **(B)** displacement of the optic nerve head (ONH) and anterior lamina cribrosa (LC) surfaces. CI = confidence interval.

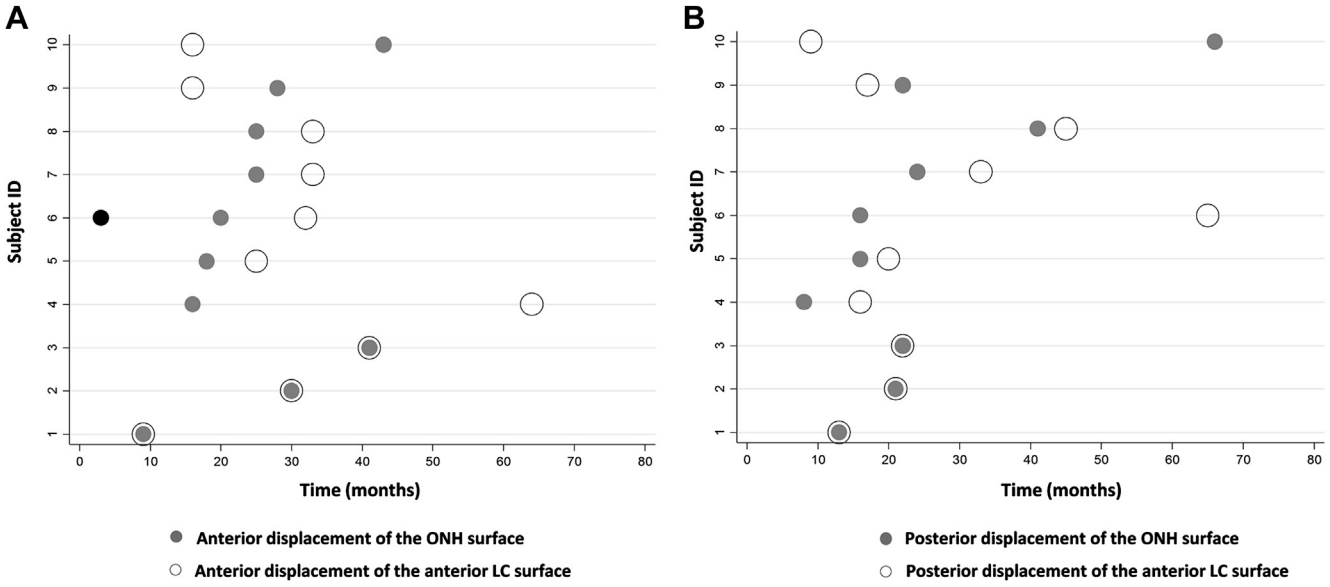

Figure 4. The sequence of change in eyes with confirmed significant anterior **(A)** and posterior **(B)** displacement of both the optic nerve head (ONH) and anterior lamina cribrosa (LC) surfaces. Among the 10 eyes with anterior displacement for the ONH and anterior LC surfaces **(A)**, 3 had optic nerve head surface depth (ONHSD) change at the same time with anterior lamina cribrosa surface depth (ALCSD) change (subjects 1–3) and 5 had ONHSD change before ALCSD change (subjects 4–8). Subject 6 (highlighted in *black dot*) had significant posterior displacement of the ONH and anterior LC surfaces before significant anterior displacement of the ONH and anterior LC surfaces. Among the 10 eyes with posterior displacement of both the ONH and anterior laminar surfaces **(B)**, 3 had ONHSD change at the same time with ALCSD change (subjects 1–3) and 5 had ONHSD change before ALCSD change (subjects 4–8). ID = identification.

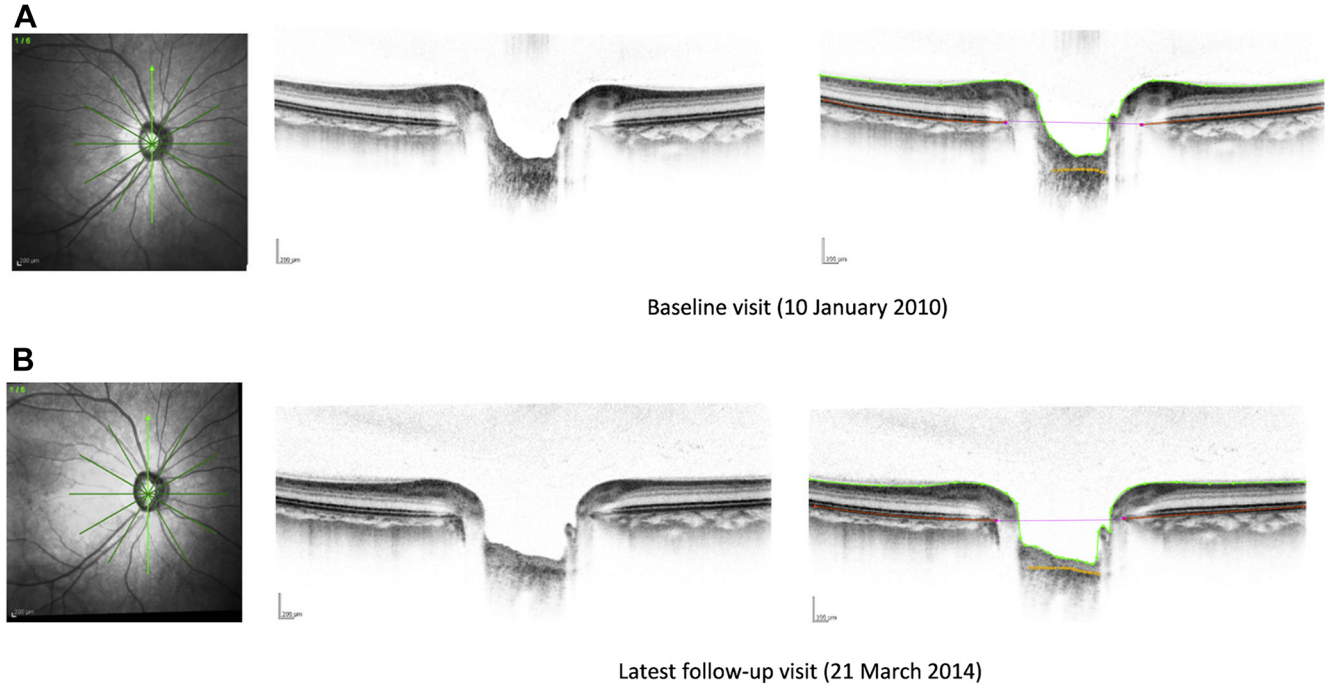

Figure 5. An example demonstrating posterior displacement of the optic nerve head (ONH) and anterior lamina cribrosa (LC) surfaces in a glaucomatous eye followed from January 10, 2010, to March 21, 2014. The scanning laser ophthalmoscopy image and optical coherence tomography (OCT) images of the vertical meridian (with and without tracing of the reference line [*pink*], ONH [*green*], and anterior LC [*orange*] surfaces) at the baseline **(A)** and latest **(B)** follow-up visits are shown. The ONH and the anterior LC surfaces displaced posteriorly by 38.3 μm and 53.2 μm, respectively. The prelaminar tissue thickness (PTT) decreased by 31.9 μm. The average intraocular pressure (IOP) and the standard deviation of IOP during the follow-up were 25.5 mmHg and 5.5 mmHg, respectively.

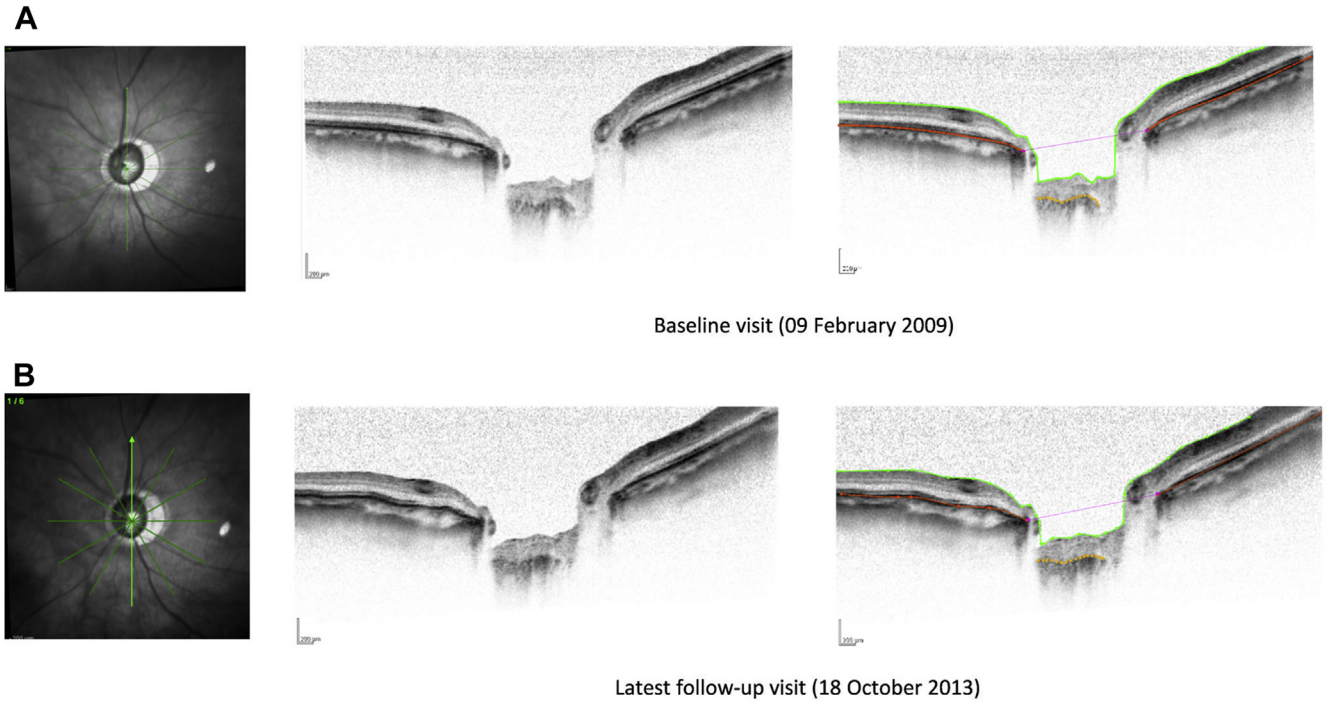

Figure 6. An example demonstrating anterior displacement of the optic nerve head (ONH) and anterior lamina cribrosa (LC) surfaces in a glaucomatous eye followed from February 9, 2009, to October 18, 2013. The scanning laser ophthalmoscopy image and optical coherence tomography (OCT) images of the vertical meridian (with and without manual tracing of the reference line [*pink*], ONH [*green*], and anterior LC [*orange*] surfaces) at the baseline **(A)** and latest **(B)** follow-up visits are shown. The ONH and the anterior LC surfaces displaced anteriorly by 41.0 μm and 59.3 μm, respectively. The prelaminar tissue thickness (PTT) did not show a significant change. The average intraocular pressure (IOP) and the standard deviation of IOP during the follow-up were 20.1 mmHg and 1.3 mmHg, respectively.

Specificity of Optic Nerve Head Surface Depth, Anterior Lamina Cribrosa Surface Depth, and Prelaminar Tissue Thickness

The normal group was followed for an average of 5.1 years (range, 4.0−6.0 years). A total of 3, 6, and 2 eyes had a significant change in ONHSD, ALCSD, and PTT, respectively, and the specificity was 91.4% (95% CI, 77.6−97.0), 82.9% (95% CI, 67.3−91.9), and 94.3% (95% CI, 81.4−98.4), respectively.

Longitudinal Changes of Optic Nerve Head Surface Depth, Anterior Lamina Cribrosa Surface Depth, and Prelaminar Tissue Thickness in Glaucoma

The ranges of ONHSD and ALCSD changes (the average of the 2 latest follow-up ONHSD/ALCSD minus the average of the 2 baseline ONHSD/ALCSD) in the glaucoma group (138 eyes) were between −68.2 μm and 165.9 μm and between −108.6 μm and 168.9 μm, respectively. Figure 2A shows scatter plots of ONHSD change versus ALCSD change, and Figure 2B shows scatter plots of PTT change versus ALCSD change. By taking all eyes in the glaucoma group into consideration (n = 138), ONHSD change was positively associated with the ALCSD change ($R^2 = 0.733$, $P < 0.001$), whereas PTT change was negatively associated with the ALCSD change ($R^2 = 0.101$, $P < 0.001$). We measured and compared the distance (the best fitting curve joining the visible pixels) and the visible pixels of the anterior LC surface of individual B-scans between the baseline (900.8±207.8 μm, 19.1±4.4 pixels) and the latest (897.0±198.4 μm, 18.7±4.1 pixels) follow-up visits for all glaucomatous eyes and found no significant differences between them ($P \geq 0.560$, linear mixed modeling). Likewise, there were no significant differences in the distance and the visible pixels of the anterior LC surface between the baseline (608.6±145.2 μm, 14.5±2.7 pixels) and the latest (590.8±143.6 μm, 14.1±2.8 pixels) follow-up visits for all normal eyes ($P \geq 0.071$, linear mixed modeling).

A total of 33 eyes (23.9%) (31 patients) had confirmed ONHSD change, in which 21 (63.6%) had posterior and 12 (36.4%) had anterior displacement of the ONH surface. Confirmed ALCSD change was found in 34 eyes (24.6%) (29 patients), in which 17 (50.0%) had posterior and 17 (50.0%) had anterior displacement of the anterior LC surface. The agreement between ONHSD and ALCSD changes was moderate to substantial (Kappa = 0.655 for anterior displacement and 0.453 for posterior displacement) (Fig 3). Among the 10 eyes with anterior displacement for both the ONH and anterior LC surfaces, 8 (80%) had ONHSD change detected at the same time (n = 3) or before (n = 5) ALCSD change (Fig 4A). Among the 10 eyes with posterior displacement of both the ONH and anterior laminar surfaces, 8 (80%) had ONHSD change at the same time (n = 3) or before (n = 5) ALCSD change (Fig 4B). There was only 1 eye that showed a change in ONHSD/ALCSD in 1 direction when significant change was first detected, and then changed in the opposite direction in the latest follow-up visit. This eye had significant posterior displacement of both the ONH and anterior LC surfaces, and then anterior displacement of the ONH surface followed by anterior displacement of the anterior LC surface (Fig 4A, subject identification 6). Among the 21 eyes with confirmed posterior displacement of the ONH surface, 7 (33.3%) had thinning of the

Table 2. Comparisons of Biometric, Visual Field, Intraocular Pressure, Optic Disc, and Retinal Nerve Fiber Layer Measurements between Eyes with Anterior and Posterior Displacement of Optic Nerve Head Surface

	Anterior Displacement of ONH Surface (n = 12 eyes)	Posterior Displacement of ONH Surface (n = 21 eyes)	P Value*
Average IOP during follow-up (mmHg)	18.7±3.5	20.0±4.1	0.344
SD of IOP during follow-up (mmHg)	2.8±1.4	3.0±1.7	0.678
Baseline age (yrs)	54.8±6.9	47.3±17.1	0.300
Baseline axial length (mm)	24.9±2.1	24.9±1.8	0.935
Baseline BMO area (mm^2)	2.19±0.50	1.93±0.32	0.098
Baseline global RNFL thickness (μm)	67.3±18.6	72.8±14.9	0.336
Baseline visual field MD (dB)	−12.43±8.01	−5.93±6.78	0.017
Visual field progression (likely or possible) (No. of eyes/%)	2 (16.7%)	6 (28.6%)	0.678
Visual field progression (likely) (No. of eyes/%)	2 (16.7%)	6 (28.6%)	0.678
History of filtration surgery (No. of eyes/%)	4 (33.3%)	6 (28.6%)	1.000

BMO = Bruch's membrane opening; dB = decibels; IOP = intraocular pressure; MD = mean deviation; ONH = optic nerve head; RNFL = retinal nerve fiber layer; SD = standard deviation.
*Comparisons were performed using linear mixed modeling except for "visual field progression" and "history of filtration surgery," for which the Fisher exact test was used.

prelaminar tissue. Thirteen eyes (9.4%) showed a reduction and 3 eyes (2.2%) had an increase in PTT among the 138 eyes of the glaucoma group. Examples of posterior and anterior displacement of the ONH/anterior LC surfaces, are illustrated in Figures 5 and 6, respectively.

Differences between Anterior and Posterior Optic Nerve Head/Lamina Cribosa Surface Displacement in Glaucoma

There were no significant differences in the average IOP and SD of IOP during follow-up, axial length, BMO area, and global RNFL thickness between eyes with anterior and posterior displacement of the ONH surface and anterior LC surface ($P \geq 0.098$) (Table 2). Eyes with anterior displacement of the ONH surface had significantly worse visual field MD than those with posterior displacement ($P = 0.017$). The mean age of subjects with eyes with posterior displacement of the anterior LC surface was less than of those with anterior displacement ($P = 0.025$) (Table 3). The proportions of eyes with visual field progression and history of filtration surgery were comparable between the groups with anterior and posterior displacement of the ONH/anterior LC surfaces ($P \geq 0.678$) (Tables 2 and 3). Some 47.1% of eyes (8/17) with visual field likely progression did not show anterior/posterior displacement of the ONH and anterior LC surfaces.

Impact of Intraocular Pressure on Optic Nerve Head Surface Depth and Anterior Lamina Cribrosa Surface Depth Displacement in Glaucoma

Over a period of 5.4 years of follow-up (range, 4.0−6.4 years), the average IOP and the IOP SD of an individual eye ranged from 9.6 to 29.4 mmHg (mean, 19.1±3.0 mmHg), and 0.8 to 7.4 mmHg (mean, 2.4±1.2 mHg), respectively, in the glaucoma group. A

Table 3. Comparisons of Biometric, Visual Field, Intraocular Pressure, Optic Disc, and Retinal Nerve Fiber Layer Measurements between Eyes with Anterior and Posterior Displacement of Anterior Lamina Cribrosa Surface

	Anterior Displacement of Anterior Lamina Cribrosa Surface (n = 17 Eyes)	Posterior Displacement of Anterior Lamina Cribrosa Surface (n = 17 Eyes)	P Value*
Average IOP during follow-up (mmHg)	18.5±3.9	18.9±3.6	0.918
SD of IOP during follow-up (mmHg)	2.8±1.5	2.7±1.8	0.747
Baseline age (yrs)	54.7±8.0	43.7±14.6	0.025
Baseline axial length (mm)	24.6±1.8	25.7±1.9	0.147
Baseline BMO area (mm^2)	2.08±0.40	1.93±0.37	0.224
Baseline global RNFL thickness (μm)	65.8±20.0	73.5±13.5	0.353
Baseline visual field MD (dB)	−11.39±8.85	−7.19±8.50	0.413
Visual field progression (likely or possible) (No. of eyes/%)	2 (11.8%)	2 (11.8%)	1.000
Visual field progression (likely) (No. of eyes/%)	2 (11.8%)	2 (11.8%)	1.000
History of filtration surgery (No. of eyes/%)	6 (35.3%)	4 (23.5%)	0.708

BMO = Bruch's membrane opening; dB = decibels; IOP = intraocular pressure; MD = mean deviation; RNFL = retinal nerve fiber layer; SD = standard deviation.
*Comparisons were performed using linear mixed modeling except for "visual field progression" and "history of filtration surgery," for which the Fisher exact test was used.

Table 4. Multivariable Analysis Investigating the Association between Changes in Optic Nerve Head Surface Depth/Anterior Lamina Cribrosa Surface Depth (Mean of the Latest 2 Minus Mean of 2 Baseline Optic Nerve Head Surface Depth/Anterior Lamina Cribrosa Surface Depth Measurements) and Intraocular Pressure Measurements during the Follow-up

	ONHSD Change				ALCSD Change			
	Coefficient	*P Value*	95% CI		*Coefficient*	*P Value*	95% CI	
Average IOP during follow-up (mmHg)	1.73	0.021	0.27	3.20	2.30	0.022	0.32	4.29
Standard deviation of IOP during follow-up (mmHg)	−1.21	0.499	−4.74	2.31	−5.26	0.027	−9.92	−0.61

ALCSD = anterior lamina cribrosa surface depth; CI = confidence interval; IOP = intraocular pressure; ONHSD = optic nerve head surface depth; SD = standard deviation.

higher average IOP was significantly associated with posterior displacement of the ONH ($P = 0.021$) and anterior LC surfaces ($P = 0.023$) (Table 4). Posterior displacement of the anterior LC surface also was associated with a lower IOP SD ($P = 0.027$). The 2 factors significantly associated with both ONHSD and ALCSD changes in the multivariable model after adjustment of SD of IOP, baseline axial length, BMO area, global RNFL thickness, and history of glaucoma surgery were the average IOP during follow-up and baseline age (Table 5). For each millimeter of mercury increase in the average IOP, the ONH and anterior LC surfaces displaced posteriorly by 1.6 μm and 2.0 μm, respectively. For each year increase in the baseline age, these surfaces displaced anteriorly by 0.4 μm and 0.6 μm, respectively.

Discussion

To our knowledge, this is an original prospective study illustrating the clinical application of SD OCT to track the ONH and LC surfaces in the long-term and identify factors associated with ONH and LC deformation in patients with glaucoma. We showed that both the ONH and anterior LC surfaces deformed during the course of glaucoma progression. These surfaces displaced not only posteriorly (20.3% of eyes) (Fig 5) but also anteriorly (13.8% of eyes) (Fig 6), with IOP and baseline age independently associated with the magnitude of displacement (Table 5). An increase in the average IOP during the follow-up was associated with posterior displacement, whereas an older age at baseline was associated with a relative anterior displacement of the ONH and anterior LC surfaces. These changes likely represent chronic ONH structural changes (i.e., the plastic component of change), although it is notable that ambient IOP also may influence ONHSD and ALCSD (i.e., the elastic component of change).[27,28]

The LC is a supporting connective tissue formed by layers of interweaving skeins of collagen, elastic fibers, and astrocytes through which axons of retinal ganglion cells pass. Proposed as the primary site of optic nerve degeneration in glaucoma,[29] the LC is a strategic location for detection of glaucomatous optic disc damage. However, clinical investigation of LC deformation has been largely limited to eyes undergoing acute IOP elevation or after a large IOP reduction after filtration surgery and medical or laser treatment.[9–12,30,31] Agoumi et al[12] applied an external force through the inferior lid with an ophthalmodynamometer to elevate the IOP by a mean of 12.4 mmHg in 12 glaucomatous and 24 normal eyes and showed that the ONH surface displaced posteriorly by a mean of 15.7 μm.[12] However, the ALCSD was resistant to acute IOP elevation. After IOP reduction, Lee et al[10] reported an anterior displacement of the anterior LC surface. The ALCSD decreased from 614.58±179.57 μm to 503.90±142.67 μm in 35 glaucomatous eyes at 6 months after trabeculectomy. Similar findings were observed by Reis et al.[9] The anterior LC surface displaced anteriorly by 17.9±25.8 μm in 22 patients with glaucoma at 6 months after trabeculectomy. Other studies also have shown anterior displacement of the anterior LC surface

Table 5. Multivariable Analysis Investigating Factors Associated with the Changes in Optic Nerve Head Surface Depth/Anterior Lamina Cribrosa Surface Depth (Mean of the Latest 2 Minus Mean of 2 Baseline Optic Nerve Head Surface Depth/Anterior Lamina Cribrosa Surface Depth Measurements)

	ONHSD Change				ALCSD Change			
	Coefficient	*P Value*	95% CI		*Coefficient*	*P Value*	95% CI	
Average IOP during follow-up (mmHg)	1.57	0.029	0.16	2.97	2.02	0.038	0.12	3.94
Standard deviation of IOP during follow-up (mmHg)	−1.36	0.455	−4.91	2.21	−5.00	0.037	−9.70	−0.29
Baseline age (years)	−0.41	0.009	−0.72	−0.10	−0.64	0.003	−1.08	−0.22
Baseline axial length (mm)	−0.79	0.528	−3.24	1.68	−0.58	0.740	−3.96	−2.82
Baseline BMO area (mm^2)	−4.68	0.283	−13.19	3.85	3.02	0.610	−8.53	14.60
Baseline global RNFL thickness (μm)	0.08	0.492	−0.14	0.30	0.21	0.158	−0.08	0.51
History of filtration surgery	5.02	0.348	−5.48	15.51	2.03	0.779	−12.14	16.15

ALCSD = anterior lamina cribrosa surface depth; BMO = Bruch's membrane opening; CI = confidence interval; IOP = intraocular pressure; ONHSD = optic nerve head surface depth; RNFL = retinal nerve fiber layer; SD = standard deviation.

after a significant IOP reduction with medical or laser treatment.[11,30] These studies demonstrate displacement of the ONH and anterior laminar surfaces over a relatively short period of time (≤6 months). Although longitudinal changes in the size and shape of the LC pores have been demonstrated in patients with glaucoma,[32] chronic, progressive deformation of the LC in patients with glaucoma has not been studied.

We showed that chronic IOP increases were associated with posterior displacement of both the ONH and anterior LC surfaces. These surfaces deepened by up to 165.9 μm and 168.9 μm, respectively, over a mean of 5.4 years (Fig 2), and the degree of deepening was positively associated with the average IOP during follow-up (Tables 4 and 5). The magnitude of LC deformation is considerably greater than that predicted from mathematic modeling and experimental glaucoma in nonhuman primates.[6,13–15] Of note, the ONH and anterior LC surfaces could also migrate anteriorly by up to 68.2 μm and 108.6 μm, respectively (Fig 2). The relatively strong positive association between ONHSD and ALCSD changes ($R^2 = 0.733$) indicates that the ONH and anterior LC surfaces are both responsive to the levels of IOP during the course of follow-up. For each millimeter of mercury change in the average IOP during follow-up, the corresponding displacement was 2.0 μm for the anterior LC surface and 1.6 μm for the ONH surface, after adjustment of other covariates (Table 5). Among the 20 eyes with confirmed anterior (n = 10) or posterior (n = 10) displacement of both the ONH and anterior LC surfaces, 80% had ONH surface change detected at or before the onset of anterior LC surface displacement (Fig 4), suggesting that the ALCSD was more resistant to change compared with the ONHSD, a finding in line with the acute IOP elevation study by Agoumi et al.[12] It is interesting to note that the SD of IOP during follow-up was negatively associated with ALCSD change, and the association remained significant in the model even after excluding patients with a history of filtration surgery (n = 24) ($P < 0.001$). All patients followed in the study received some form of IOP-lowering treatment, and the initiation or augmentation of IOP-lowering therapy during the follow-up may affect the directionality of laminar deformation.

There are age-related differences in IOP responsiveness of ONHSD and ALCSD change (Table 5), which is likely related to age-related differences in LC stiffness. An older age was associated with a decrease in magnitude of posterior displacement of the ONH and anterior LC surfaces. The decreasing ALCSD with increasing age may contribute to the differences in structure function relationships between young and old patients with glaucoma.[33]

In the current study, confirmed ONHSD/ALCSD changes were defined when the differences between the first baseline and the 2 latest consecutive follow-up measurements were greater than the corresponding reproducibility coefficient. Some 20.3% and 13.8% of eyes showed posterior and anterior displacement, respectively, of the ONH and/or anterior LC surfaces. Although anterior LC displacement has been reported after filtration surgery,[9–11,31] it should be noted that the proportion of eyes with filtration surgery was not significantly different between the groups with anterior and posterior displacement of the anterior LC surface ($P = 0.708$) (Table 3). The proportion of eyes with visual field progression was also comparable between the 2 groups ($P = 1.000$) (Table 3). Can anterior displacement of the LC be associated with glaucoma progression? Although remodeling of the LC including extracellular matrix remodeling and synthesis of retrolaminar septa may contribute to its anterior displacement,[34] Crawford Downs et al[15] postulated from a mechanical perspective that there are 2 components of IOP-induced LC deformation, one acting on the anterior LC surface contributing to the posterior displacement and another acting on the sclera, which causes scleral canal expansion and tautening, or anterior displacement, of the LC. The longitudinal observation of both posterior and anterior displacement of the anterior LC surface in the current study supports this hypothesis. Anterior scleral canal wall expansion was first described by Bellezza et al[35] in pressurized (IOP, 10 mmHg) and nonpressurized (IOP, 0 mmHg) normal monkey eyes.[35] With finite element modeling, Sigal[36] and Sigal et al[37] showed that scleral properties had a strong influence on ONH mechanical response and that scleral canal expansion was detected with simulated IOP elevation. The directionality of LC deformation is likely a consequence of a complex interaction among the IOP (and possibly the retrolaminar intracranial pressure), the geometry, and the biomechanical properties of the LC and the surrounding sclera. Alternatively, the apparent anterior displacement of the LC could represent a confound secondary to peripapillary choroidal thinning, which may occur faster in older eyes.[38]

Lamina cribrosa deformation has been shown to be evident before RNFL thinning in nonhuman primates induced with experimental glaucoma.[5,8] Thus, detecting LC deformation may serve as an early indicator for therapeutic intervention before irreversible loss of RNFL and visual function. Nevertheless, it is notable that a significant proportion of eyes (47.1%) that developed visual field progression during follow-up in this study did not have observable ONH/LC displacement. Although progressive ONHSD and ALCSD changes could have occurred before the recruitment, the possibility of a relatively low sensitivity for detection of ONH and anterior LC surface change cannot be excluded (of note, confirmed ONHSD/ALCSD change had to be greater than the corresponding reproducibility coefficient for the latest 2 consecutive follow-up visits). Alternatively, these eyes may contain a stiffer LC that was more resistant to IOP. Factors other than IOP and LC deformation may contribute to glaucoma progression.

The proportion of eyes with prelaminar tissue thickening (2.2%) and thinning (9.4%) was relatively small. Because PTT is generally smaller than ONHSD and ALCSD, detecting significant change in PTT could be challenging (the reproducibility coefficient of PTT [24.8 μm] was greater than that of ONHSD [18.0 μm] and ALCSD [23.4 μm]). Because posterior deformation of the ONH surface could be secondary to prelaminar tissue loss without concomitant deformation of the anterior LC surface, we

noticed that the agreement between ONH surface change and anterior laminar surface change was weaker for the posterior (kappa = 0.453) than the anterior (kappa = 0.655) displacement (Fig 3). Although prelaminar tissue thinning can be related to the loss of prelaminar neuronal tissue, reduction in PTT after acute IOP elevation has been reported in nonhuman primates,[28] indicating that ambient IOP can directly influence PTT. That PTT decreases before RNFL loss in experimental glaucoma (measured under manometric IOP control) also suggests the involvement of connective tissue remodeling in the prelaminar tissue.[5] Prelaminar tissue thickening has been described in nonhuman primates with experimental glaucoma,[39] which can be consequential to blockage of orthograde axoplasmic transport within the axons of retinal ganglion cells, gliosis, and connective tissue remodeling.[34,40,41] The relative contribution of neuronal tissue loss and glial tissue deposition in determining the change in PTT and its significance in glaucoma progression remain to be determined.

Study Strengths and Limitations

One strength of our study is the inclusion of a large volume of OCT scans spanning over a relatively long period (a mean of 5.3 years) for change analysis. The adoption of eye tracking and image registration for OCT imaging in all of the follow-up visits considerably decreased the test−retest variability of the OCT measurements. Confirming significant ONHSD/ALCSD/PTT changes with 2 consecutive follow-up visits ensured a high specificity in the change analysis but at the expense of underestimating the number of changes. The sensitivity for detection of change could be adversely affected. B-scans required meticulous manual segmentation, which posed a major barrier to high-volume measurement, and we only managed to analyze 6 B-scans for each eye in each visit. This may reduce the capacity to measure and detect ONHSD/ALCSD/PTT change. Focal changes could be missed. In addition, all the measurements were done in only 2 dimensions, which increases variability and reduces accuracy. Yet, it is worth noting that the scan pattern (raster vs. radial scans) and number of B-scans analyzed for measurement of average ONHSD/ALCSD vary widely among published studies.

Our analysis also suffered from limitations universal to studies measuring ONHSD and ALCSD with OCT. These include incomplete visualization of the anterior LC surface (ALCSD and PTT were measured with reference to the locations where the anterior LC surface was visible in the B-scans) and the assumption of a stable reference line during the follow-up. A significant proportion of normal eyes had undetectable anterior LC surface because of thick neuroretinal rim and small optic cups in at least 1 B-scan in the follow-up image series. Our finding may not be generalized to eyes with early ONH damage. The finding that the distance and pixels of visible anterior LC surface in individual B-scans were comparable between the baseline and latest follow-up visits suggests that our ALCSD measurement was unlikely to be affected by potential changes in the visibility of peripheral LC during the follow-up period. In this study, measurements of ONHSD and ALCSD were performed with reference to the BMO. We selected a BMO-based reference line because the BMO is a common anatomic reference for measurement of ONHSD and ALCSD. Reference planes based on anatomic locations other than BMO have been examined, but none has been shown to be superior to the BMO reference plane. He et al[8] compared the BMO reference plane with another reference plane based on the best-fitting ellipse through retinal pigment epithelium/Bruch's membrane complex points located at a 1500 μm radius from the BMO centroid along the BMO plane for measurement of ALCSD and found that the BMO reference plane had superior sensitivity and specificity for detection of glaucoma onset. Reis et al[9] measured postsurgical anterior laminar displacement using the BMO reference plane and a reference plane based on the peripheral internal limiting membrane similar to the reference ring used in confocal scanning laser ophthalmoscopy, and showed almost identical results. They reported that there were no nonuniform measurement differences in these 2 reference planes. In a recent cross-sectional study, Johnstone et al[38] demonstrated that peripapillary choroidal thickness was negatively correlated with age and that BMO height, measured with reference to a scleral reference plane, was smaller in older individuals. Although it is plausible that BMO could migrate posteriorly with age consequential to age-related choroidal thinning, which may in turn affect the measurement of ONHSD and ALCSD changes, longitudinal data confirming this observation are lacking. Because our OCT volumes are composed of non−EDI B-scans, it would be difficult to detect the anterior scleral surface for measurement of ONHSD/ALCSD. By connecting 2 peripheral points of the retinal pigment epithelium/Bruch's membrane at 15° on either side of the ONH to define the reference plane, Fortune et al[42] showed that the depth of BMO centroid increased by more than 40 μm relative to the reference plane after acute elevation of IOP. Further investigation is needed to measure the longitudinal changes of the peripapillary choroidal thickness in glaucomatous eyes and evaluate whether the BMO is anatomically stable over time.

It is worth mentioning that the BMO area estimated from automated BMO segmentation in the Cirrus HD-OCT is likely to be different from that measured with manual detection in the Spectralis OCT. However, this difference is unlikely to affect the comparison of BMO area between eyes with anterior and posterior displacement of ONH/anterior LC surfaces (Tables 2 and 3). Of note, IOP was assumed to be linearly related to ONHSD and ALCSD in our linear mixed model analysis, but the effect of IOP on the ONH and LC surfaces could be nonlinear. Last, results from this study may not be generalized to other populations. We included patients with glaucoma with different degrees of glaucomatous damage, and all patients were Chinese. The degree to which ONHSD and ALCSD change in response to IOP and other biometric variables may vary among different ethnic groups and different degrees of ONH damage.

To summarize, posterior, as well as anterior, displacement of the ONH and anterior LC surfaces was observed in a significant portion of patients with glaucoma during longitudinal

follow-up. Intraocular pressure was positively and age was negatively associated with changes in ONHSD and ALCSD. Approximately half of the eyes with visual field "likely progression" did not have a change in ONHSD/ALCSD. Additional studies are ongoing to investigate the impact of ocular biomechanical response on detection of ONH/LC deformation and optic nerve degeneration in glaucoma.

References

1. Vilupuru AS, Rangaswamy NV, Frishman LJ, et al. Adaptive optics scanning laser ophthalmoscopy for in vivo imaging of lamina cribrosa. J Opt Soc Am A Opt Image Sci Vis 2007;24:1417–25.
2. Kim TW, Kagemann L, Girard MJ, et al. Imaging of the lamina cribrosa in glaucoma: perspectives of pathogenesis and clinical applications. Curr Eye Res 2013;38:903–9.
3. Nadler Z, Wang B, Wollstein G, et al. Repeatability of in vivo 3D lamina cribrosa microarchitecture using adaptive optics spectral domain optical coherence tomography. Biomed Opt Express 2014;5:1114–23.
4. Strouthidis NG, Grimm J, Williams GA, et al. A comparison of optic nerve head morphology viewed by spectral domain optical coherence tomography and by serial histology. Invest Ophthalmol Vis Sci 2010;51:1464–74.
5. Strouthidis NG, Fortune B, Yang H, et al. Longitudinal change detected by spectral domain optical coherence tomography in the optic nerve head and peripapillary retina in experimental glaucoma. Invest Ophthalmol Vis Sci 2011;52:1206–19.
6. Yang H, Thompson H, Roberts MD, et al. Deformation of the early glaucomatous monkey optic nerve head connective tissue after acute IOP elevation in 3-D histomorphometric reconstructions. Invest Ophthalmol Vis Sci 2011;52:345–63.
7. Yang H, Williams G, Downs JC, et al. Posterior (outward) migration of the lamina cribrosa and early cupping in monkey experimental glaucoma. Invest Ophthalmol Vis Sci 2011;52:7109–21.
8. He L, Yang H, Gardiner SK, et al. Longitudinal detection of optic nerve head changes by spectral domain optical coherence tomography in early experimental glaucoma. Invest Ophthalmol Vis Sci 2014;55:574–86.
9. Reis AS, O'Leary N, Stanfield MJ, et al. Laminar displacement and prelaminar tissue thickness change after glaucoma surgery imaged with optical coherence tomography. Invest Ophthalmol Vis Sci 2012;53:5819–26.
10. Lee EJ, Kim TW, Weinreb RN. Reversal of lamina cribrosa displacement and thickness after trabeculectomy in glaucoma. Ophthalmology 2012;119:1359–66.
11. Lee EJ, Kim TW, Weinreb RN, et al. Reversal of lamina cribrosa displacement after intraocular pressure reduction in open-angle glaucoma. Ophthalmology 2013;120:553–9.
12. Agoumi Y, Sharpe GP, Hutchison DM, et al. Laminar and prelaminar tissue displacement during intraocular pressure elevation in glaucoma patients and healthy controls. Ophthalmology 2011;118:52–9.
13. Sigal IA, Flanagan JG, Tertinegg I, et al. Predicted extension, compression and shearing of optic nerve head tissues. Exp Eye Res 2007;85:312–22.
14. Sigal IA, Flanagan JG, Tertinegg I, et al. Modeling individual-specific human optic nerve head biomechanics. Part I: IOP-induced deformations and influence of geometry. Biomech Model Mechanobiol 2009;8:85–98.
15. Crawford Downs J, Roberts MD, Sigal IA. Glaucomatous cupping of the lamina cribrosa: a review of the evidence for active progressive remodeling as a mechanism. Exp Eye Res 2011;93:133–40.
16. Spaide RF, Koizumi H, Pozzoni MC. Enhanced depth imaging spectral-domain optical coherence tomography. Am J Ophthalmol 2008;146:496–500.
17. Sharma A, Oakley JD, Schiffman JC, et al. Comparison of automated analysis of Cirrus HD OCT spectral-domain optical coherence tomography with stereo photographs of the optic disc. Ophthalmology 2011;118:1348–57.
18. British Standards Institution. Precision of Test Methods 1: Guide for the Determination and Reproducibility for a Standard Test Method (BS 597, Part 1). London: British Standards Institution; 1975.
19. Bland JM, Altman DG. Measurement error. BMJ 1996;313:744.
20. Heijl A, Leske MC, Bengtsson B, et al; EMGT Group. Measuring visual field progression in the Early Manifest Glaucoma Trial. Acta Ophthalmol Scand 2003;81:286–93.
21. Kotecha A, Crabb DP, Spratt A, et al. The relationship between diurnal variations in intraocular pressure measurements and central corneal thickness and corneal hysteresis. Invest Ophthalmol Vis Sci 2009;50:4229–36.
22. Hager A, Loge K, Schroeder B, et al. Effect of central corneal thickness and corneal hysteresis on tonometry as measured by dynamic contour tonometry, ocular response analyzer, and Goldmann tonometry in glaucomatous eyes. J Glaucoma 2008;17:361–5.
23. Pepose JS, Feigenbaum SK, Qazi MA, et al. Changes in corneal biomechanics and intraocular pressure following LASIK using static, dynamic, and noncontact tonometry. Am J Ophthalmol 2007;143:39–47.
24. Kaufmann C, Bachmann LM, Thiel MA. Intraocular pressure measurements using dynamic contour tonometry after laser in situ keratomileusis. Invest Ophthalmol Vis Sci 2003;44:3790–4.
25. Landis JR, Koch GG. The measurement of observer agreement for categorical data. Biometrics 1977;33:159–74.
26. Nakagawa S, Schielzeth H. A general and simple method for obtaining R^2 from generalized linear mixed-effects models. Methods in Ecology and Evolution 2013;4:133–42.
27. Fatehee N, Yu PK, Morgan WH, et al. The impact of acutely elevated intraocular pressure on the porcine optic nerve head. Invest Ophthalmol Vis Sci 2011;52:6192–8.
28. Strouthidis NG, Fortune B, Yang H, et al. Effect of acute intraocular pressure elevation on the monkey optic nerve head as detected by spectral domain optical coherence tomography. Invest Ophthalmol Vis Sci 2011;52:9431–7.
29. Quigley HA, Addicks EM, Green WR, et al. Optic nerve damage in human glaucoma. II. The site of injury and susceptibility to damage. Arch Ophthalmol 1981;99:635–49.
30. Park HY, Shin HY, Jung KI, et al. Changes in the lamina and prelamina after intraocular pressure reduction in patients with primary open-angle glaucoma and acute primary angle-closure. Invest Ophthalmol Vis Sci 2014;55:233–9.
31. Barrancos C, Rebolleda G, Oblanca N, et al. Changes in lamina cribrosa and prelaminar tissue after deep sclerectomy. Eye (Lond) 2014;28:58–65.
32. Tezel G, Trinkaus K, Wax MB. Alterations in the morphology of lamina cribrosa pores in glaucomatous eyes. Br J Ophthalmol 2004;88:251–6.
33. Ren R, Yang H, Gardiner SK, et al. Anterior lamina cribrosa surface depth, age, and visual field sensitivity in the Portland Progression Project. Invest Ophthalmol Vis Sci 2014;55:1531–9.

34. Hernandez MR. The optic nerve head in glaucoma: role of astrocytes in tissue remodeling. Prog Retin Eye Res 2000;19:297–321.
35. Bellezza AJ, Rintalan CJ, Thompson HW, et al. Anterior scleral canal geometry in pressurised (IOP 10) and non-pressurised (IOP 0) normal monkey eyes. Br J Ophthalmol 2003;87:1284–90.
36. Sigal IA. Interactions between geometry and mechanical properties on the optic nerve head. Invest Ophthalmol Vis Sci 2009;50:2785–95.
37. Sigal IA, Yang H, Roberts MD, et al. IOP-induced lamina cribrosa displacement and scleral canal expansion: an analysis of factor interactions using parameterized eye-specific models. Invest Ophthalmol Vis Sci 2011;52:1896–907.
38. Johnstone J, Fazio M, Rojananuangnit K, et al. Variation of the axial location of Bruch's membrane opening with age, choroidal thickness, and race. Invest Ophthalmol Vis Sci 2014;55:2004–9.
39. Yang H, Downs JC, Bellezza A, et al. 3-D histomorphometry of the normal and early glaucomatous monkey optic nerve head: prelaminar neural tissues and cupping. Invest Ophthalmol Vis Sci 2007;48:5068–84.
40. Anderson DR, Hendrickson A. Effect of intraocular pressure on rapid axoplasmic transport in monkey optic nerve. Invest Ophthalmol 1974;13:771–83.
41. Quigley HA, Addicks EM. Chronic experimental glaucoma in primates. II. Effect of extended intraocular pressure elevation on optic nerve head and axonal transport. Invest Ophthalmol Vis Sci 1980;19:137–52.
42. Fortune B, Yang H, Strouthidis NG, et al. The effect of acute intraocular pressure elevation on peripapillary retinal thickness, retinal nerve fiber layer thickness, and retardance. Invest Ophthalmol Vis Sci 2009;50:4719–26.

Footnotes and Financial Disclosures

Originally received: May 25, 2014.
Final revision: February 24, 2015.
Accepted: February 26, 2015.
Available online: May 9, 2015. Manuscript no. 2014-803.

[1] Department of Ophthalmology and Visual Sciences, The Chinese University of Hong Kong, Hong Kong, PRC.

[2] Hamilton Glaucoma Center and the Shiley Eye Center, Department of Ophthalmology, University of California, San Diego, California.

[3] Department of Mathematics and Statistics, Hang Seng Management College, Siu Lek Yuen, Hong Kong.

Financial Disclosure(s):
The author(s) have made the following disclosure(s): C.K.S.L.: Speaker honorarium − Carl Zeiss Meditec, Heidelberg Engineering, Global Vision; Research support − Carl Zeiss Meditec, Optovue; Consultant fees − Alcon, Allergan; Grants/grants pending −Alcon; payment for service on speakers bureaus −Alcon, Allergan, Oculus, Santen, Tomey.

R.N.W.: Consultant − Topcon, Allergan, Aquesys, Bausch & Lomb, Zeiss; Research support − Carl Zeiss Meditec, Heidelberg Engineering, Optovue, Topcon, Nidek.

Funded by The Chinese University of Hong Kong.

Author Contributions:

Conception and design: Weinreb, Leung

Data collection: Wu, Xu, Leung

Analysis and interpretation: Wu, Xu, Yu, Leung

Obtained funding: Not applicable

Overall responsibility: Wu, Xu, Weinreb, Yu, Leung

Abbreviations and Acronyms:
ALCSD = anterior lamina cribrosa surface depth; **BMO** = Bruch's membrane opening; **CI** = confidence interval; **DCT** = dynamic contour tonometer; **EDI** = enhanced-depth imaging; **IOP** = intraocular pressure; **OCT** = optical coherence tomography; **ONH** = optic nerve head; **ONHSD** = optic nerve head surface depth; **PTT** = prelaminar tissue thickness; **RNFL** = retinal nerve fiber layer; **SD** = standard deviation; **SD OCT** = spectral-domain optical coherence tomography.

Correspondence:
Christopher K.S. Leung, MD, MB, ChB, Department of Ophthalmology and Visual Sciences, The Chinese University of Hong Kong, Hong Kong, PRC. E-mail: tlims00@hotmail.com.